Search for lepton-number violating processes in B^{+}→h^{-}l^{+}l^{+} decays

J. P. Lees *et al.* (BABAR Collaboration)

Phys. Rev. D **85**, 071103 — Published 19 April 2012

DOI: 10.1103/PhysRevD.85.071103

Search for lepton-number violating processes in $B^+ \to h^-\ell^+\ell^+$ decays

J. P. Lees,[1] V. Poireau,[1] V. Tisserand,[1] J. Garra Tico,[2] E. Grauges,[2] A. Palano[ab],[3] G. Eigen,[4] B. Stugu,[4] D. N. Brown,[5] L. T. Kerth,[5] Yu. G. Kolomensky,[5] G. Lynch,[5] H. Koch,[6] T. Schroeder,[6] D. J. Asgeirsson,[7] C. Hearty,[7] T. S. Mattison,[7] J. A. McKenna,[7] A. Khan,[8] V. E. Blinov,[9] A. R. Buzykaev,[9] V. P. Druzhinin,[9] V. B. Golubev,[9] E. A. Kravchenko,[9] A. P. Onuchin,[9] S. I. Serednyakov,[9] Yu. I. Skovpen,[9] E. P. Solodov,[9] K. Yu. Todyshev,[9] A. N. Yushkov,[9] M. Bondioli,[10] D. Kirkby,[10] A. J. Lankford,[10] M. Mandelkern,[10] H. Atmacan,[11] J. W. Gary,[11] F. Liu,[11] O. Long,[11] G. M. Vitug,[11] C. Campagnari,[12] T. M. Hong,[12] D. Kovalskyi,[12] J. D. Richman,[12] C. A. West,[12] A. M. Eisner,[13] J. Kroseberg,[13] W. S. Lockman,[13] A. J. Martinez,[13] B. A. Schumm,[13] A. Seiden,[13] D. S. Chao,[14] C. H. Cheng,[14] B. Echenard,[14] K. T. Flood,[14] D. G. Hitlin,[14] P. Ongmongkolkul,[14] F. C. Porter,[14] A. Y. Rakitin,[14] R. Andreassen,[15] Z. Huard,[15] B. T. Meadows,[15] M. D. Sokoloff,[15] L. Sun,[15] P. C. Bloom,[16] W. T. Ford,[16] A. Gaz,[16] U. Nauenberg,[16] J. G. Smith,[16] S. R. Wagner,[16] R. Ayad,[17,*] W. H. Toki,[17] B. Spaan,[18] K. R. Schubert,[19] R. Schwierz,[19] D. Bernard,[20] M. Verderi,[20] P. J. Clark,[21] S. Playfer,[21] D. Bettoni[a],[22] C. Bozzi[a],[22] R. Calabrese[ab],[22] G. Cibinetto[ab],[22] E. Fioravanti[ab],[22] I. Garzia[ab],[22] E. Luppi[ab],[22] M. Munerato[ab],[22] M. Negrini[ab],[22] L. Piemontese[a],[22] V. Santoro[a],[22] R. Baldini-Ferroli,[23] A. Calcaterra,[23] R. de Sangro,[23] G. Finocchiaro,[23] P. Patteri,[23] I. M. Peruzzi,[23,†] M. Piccolo,[23] M. Rama,[23] A. Zallo,[23] R. Contri[ab],[24] E. Guido[ab],[24] M. Lo Vetere[ab],[24] M. R. Monge[ab],[24] S. Passaggio[a],[24] C. Patrignani[ab],[24] E. Robutti[a],[24] B. Bhuyan,[25] V. Prasad,[25] C. L. Lee,[26] M. Morii,[26] A. J. Edwards,[27] A. Adametz,[28] U. Uwer,[28] H. M. Lacker,[29] T. Lueck,[29] P. D. Dauncey,[30] P. K. Behera,[31] U. Mallik,[31] C. Chen,[32] J. Cochran,[32] W. T. Meyer,[32] S. Prell,[32] A. E. Rubin,[32] A. V. Gritsan,[33] Z. J. Guo,[33] N. Arnaud,[34] M. Davier,[34] D. Derkach,[34] G. Grosdidier,[34] F. Le Diberder,[34] A. M. Lutz,[34] B. Malaescu,[34] P. Roudeau,[34] M. H. Schune,[34] A. Stocchi,[34] G. Wormser,[34] D. J. Lange,[35] D. M. Wright,[35] C. A. Chavez,[36] J. P. Coleman,[36] J. R. Fry,[36] E. Gabathuler,[36] D. E. Hutchcroft,[36] D. J. Payne,[36] C. Touramanis,[36] A. J. Bevan,[37] F. Di Lodovico,[37] R. Sacco,[37] M. Sigamani,[37] G. Cowan,[38] D. N. Brown,[39] C. L. Davis,[39] A. G. Denig,[40] M. Fritsch,[40] W. Gradl,[40] K. Griessinger,[40] A. Hafner,[40] E. Prencipe,[40] D. Bailey,[41] R. J. Barlow,[41,‡] G. Jackson,[41] G. D. Lafferty,[41] E. Behn,[42] R. Cenci,[42] B. Hamilton,[42] A. Jawahery,[42] D. A. Roberts,[42] C. Dallapiccola,[43] R. Cowan,[44] D. Dujmic,[44] G. Sciolla,[44] R. Cheaib,[45] D. Lindemann,[45] P. M. Patel,[45] S. H. Robertson,[45] P. Biassoni[ab],[46] N. Neri[a],[46] F. Palombo[ab],[46] S. Stracka[ab],[46] L. Cremaldi,[47] R. Godang,[47,§] R. Kroeger,[47] P. Sonnek,[47] D. J. Summers,[47] X. Nguyen,[48] M. Simard,[48] P. Taras,[48] G. De Nardo[ab],[49] D. Monorchio[ab],[49] G. Onorato[ab],[49] C. Sciacca[ab],[49] M. Martinelli,[50] G. Raven,[50] C. P. Jessop,[51] J. M. LoSecco,[51] W. F. Wang,[51] K. Honscheid,[52] R. Kass,[52] J. Brau,[53] R. Frey,[53] N. B. Sinev,[53] D. Strom,[53] E. Torrence,[53] E. Feltresi[ab],[54] N. Gagliardi[ab],[54] M. Margoni[ab],[54] M. Morandin[a],[54] M. Posocco[a],[54] M. Rotondo[a],[54] G. Simi[a],[54] F. Simonetto[ab],[54] R. Stroili[ab],[54] S. Akar,[55] E. Ben-Haim,[55] M. Bomben,[55] G. R. Bonneaud,[55] H. Briand,[55] G. Calderini,[55] J. Chauveau,[55] O. Hamon,[55] Ph. Leruste,[55] G. Marchiori,[55] J. Ocariz,[55] S. Sitt,[55] M. Biasini[ab],[56] E. Manoni[ab],[56] S. Pacetti[ab],[56] A. Rossi[ab],[56] C. Angelini[ab],[57] G. Batignani[ab],[57] S. Bettarini[ab],[57] M. Carpinelli[ab],[57,¶] G. Casarosa[ab],[57] A. Cervelli[ab],[57] F. Forti[ab],[57] M. A. Giorgi[ab],[57] A. Lusiani[ac],[57] B. Oberhof[ab],[57] E. Paoloni[ab],[57] A. Perez[a],[57] G. Rizzo[ab],[57] J. J. Walsh[a],[57] D. Lopes Pegna,[58] J. Olsen,[58] A. J. S. Smith,[58] A. V. Telnov,[58] F. Anulli[a],[59] R. Faccini[ab],[59] F. Ferrarotto[a],[59] F. Ferroni[ab],[59] M. Gaspero[ab],[59] L. Li Gioi[a],[59] M. A. Mazzoni[a],[59] G. Piredda[a],[59] C. Bünger,[60] O. Grünberg,[60] T. Hartmann,[60] T. Leddig,[60] H. Schröder,[60] C. Voss,[60] R. Waldi,[60] T. Adye,[61] E. O. Olaiya,[61] F. F. Wilson,[61] S. Emery,[62] G. Hamel de Monchenault,[62] G. Vasseur,[62] Ch. Yèche,[62] D. Aston,[63] D. J. Bard,[63] R. Bartoldus,[63] C. Cartaro,[63] M. R. Convery,[63] J. Dorfan,[63] G. P. Dubois-Felsmann,[63] W. Dunwoodie,[63] M. Ebert,[63] R. C. Field,[63] M. Franco Sevilla,[63] B. G. Fulsom,[63] A. M. Gabareen,[63] M. T. Graham,[63] P. Grenier,[63] C. Hast,[63] W. R. Innes,[63] M. H. Kelsey,[63] P. Kim,[63] M. L. Kocian,[63] D. W. G. S. Leith,[63] P. Lewis,[63] B. Lindquist,[63] S. Luitz,[63] V. Luth,[63] H. L. Lynch,[63] D. B. MacFarlane,[63] D. R. Muller,[63] H. Neal,[63] S. Nelson,[63] M. Perl,[63] T. Pulliam,[63] B. N. Ratcliff,[63] A. Roodman,[63] A. A. Salnikov,[63] R. H. Schindler,[63] A. Snyder,[63] D. Su,[63] M. K. Sullivan,[63] J. Va'vra,[63] A. P. Wagner,[63] W. J. Wisniewski,[63] M. Wittgen,[63] D. H. Wright,[63] H. W. Wulsin,[63] C. C. Young,[63] V. Ziegler,[63] W. Park,[64] M. V. Purohit,[64] R. M. White,[64] J. R. Wilson,[64] A. Randle-Conde,[65] S. J. Sekula,[65] M. Bellis,[66] J. F. Benitez,[66] P. R. Burchat,[66] T. S. Miyashita,[66] M. S. Alam,[67] J. A. Ernst,[67] R. Gorodeisky,[68] N. Guttman,[68] D. R. Peimer,[68] A. Soffer,[68] P. Lund,[69] S. M. Spanier,[69] R. Eckmann,[70] J. L. Ritchie,[70] A. M. Ruland,[70] R. F. Schwitters,[70] B. C. Wray,[70] J. M. Izen,[71] X. C. Lou,[71] F. Bianchi[ab],[72] D. Gamba[ab],[72] L. Lanceri[ab],[73] L. Vitale[ab],[73] F. Martinez-Vidal,[74] A. Oyanguren,[74] H. Ahmed,[75] J. Albert,[75] Sw. Banerjee,[75] F. U. Bernlochner,[75] H. H. F. Choi,[75] G. J. King,[75] R. Kowalewski,[75] M. J. Lewczuk,[75] I. M. Nugent,[75] J. M. Roney,[75] R. J. Sobie,[75] N. Tasneem,[75] T. J. Gershon,[76] P. F. Harrison,[76] T. E. Latham,[76] E. M. T. Puccio,[76] H. R. Band,[77] S. Dasu,[77] Y. Pan,[77] R. Prepost,[77] and S. L. Wu[77]

(The *BABAR* Collaboration)

[1] *Laboratoire d'Annecy-le-Vieux de Physique des Particules (LAPP), Université de Savoie, CNRS/IN2P3, F-74941 Annecy-Le-Vieux, France*
[2] *Universitat de Barcelona, Facultat de Fisica, Departament ECM, E-08028 Barcelona, Spain*
[3] *INFN Sezione di Bari[a]; Dipartimento di Fisica, Università di Bari[b], I-70126 Bari, Italy*
[4] *University of Bergen, Institute of Physics, N-5007 Bergen, Norway*
[5] *Lawrence Berkeley National Laboratory and University of California, Berkeley, California 94720, USA*
[6] *Ruhr Universität Bochum, Institut für Experimentalphysik 1, D-44780 Bochum, Germany*
[7] *University of British Columbia, Vancouver, British Columbia, Canada V6T 1Z1*
[8] *Brunel University, Uxbridge, Middlesex UB8 3PH, United Kingdom*
[9] *Budker Institute of Nuclear Physics, Novosibirsk 630090, Russia*
[10] *University of California at Irvine, Irvine, California 92697, USA*
[11] *University of California at Riverside, Riverside, California 92521, USA*
[12] *University of California at Santa Barbara, Santa Barbara, California 93106, USA*
[13] *University of California at Santa Cruz, Institute for Particle Physics, Santa Cruz, California 95064, USA*
[14] *California Institute of Technology, Pasadena, California 91125, USA*
[15] *University of Cincinnati, Cincinnati, Ohio 45221, USA*
[16] *University of Colorado, Boulder, Colorado 80309, USA*
[17] *Colorado State University, Fort Collins, Colorado 80523, USA*
[18] *Technische Universität Dortmund, Fakultät Physik, D-44221 Dortmund, Germany*
[19] *Technische Universität Dresden, Institut für Kern- und Teilchenphysik, D-01062 Dresden, Germany*
[20] *Laboratoire Leprince-Ringuet, Ecole Polytechnique, CNRS/IN2P3, F-91128 Palaiseau, France*
[21] *University of Edinburgh, Edinburgh EH9 3JZ, United Kingdom*
[22] *INFN Sezione di Ferrara[a]; Dipartimento di Fisica, Università di Ferrara[b], I-44100 Ferrara, Italy*
[23] *INFN Laboratori Nazionali di Frascati, I-00044 Frascati, Italy*
[24] *INFN Sezione di Genova[a]; Dipartimento di Fisica, Università di Genova[b], I-16146 Genova, Italy*
[25] *Indian Institute of Technology Guwahati, Guwahati, Assam, 781 039, India*
[26] *Harvard University, Cambridge, Massachusetts 02138, USA*
[27] *Harvey Mudd College, Claremont, California 91711*
[28] *Universität Heidelberg, Physikalisches Institut, Philosophenweg 12, D-69120 Heidelberg, Germany*
[29] *Humboldt-Universität zu Berlin, Institut für Physik, Newtonstr. 15, D-12489 Berlin, Germany*
[30] *Imperial College London, London, SW7 2AZ, United Kingdom*
[31] *University of Iowa, Iowa City, Iowa 52242, USA*
[32] *Iowa State University, Ames, Iowa 50011-3160, USA*
[33] *Johns Hopkins University, Baltimore, Maryland 21218, USA*
[34] *Laboratoire de l'Accélérateur Linéaire, IN2P3/CNRS et Université Paris-Sud 11, Centre Scientifique d'Orsay, B. P. 34, F-91898 Orsay Cedex, France*
[35] *Lawrence Livermore National Laboratory, Livermore, California 94550, USA*
[36] *University of Liverpool, Liverpool L69 7ZE, United Kingdom*
[37] *Queen Mary, University of London, London, E1 4NS, United Kingdom*
[38] *University of London, Royal Holloway and Bedford New College, Egham, Surrey TW20 0EX, United Kingdom*
[39] *University of Louisville, Louisville, Kentucky 40292, USA*
[40] *Johannes Gutenberg-Universität Mainz, Institut für Kernphysik, D-55099 Mainz, Germany*
[41] *University of Manchester, Manchester M13 9PL, United Kingdom*
[42] *University of Maryland, College Park, Maryland 20742, USA*
[43] *University of Massachusetts, Amherst, Massachusetts 01003, USA*
[44] *Massachusetts Institute of Technology, Laboratory for Nuclear Science, Cambridge, Massachusetts 02139, USA*
[45] *McGill University, Montréal, Québec, Canada H3A 2T8*
[46] *INFN Sezione di Milano[a]; Dipartimento di Fisica, Università di Milano[b], I-20133 Milano, Italy*
[47] *University of Mississippi, University, Mississippi 38677, USA*
[48] *Université de Montréal, Physique des Particules, Montréal, Québec, Canada H3C 3J7*
[49] *INFN Sezione di Napoli[a]; Dipartimento di Scienze Fisiche, Università di Napoli Federico II[b], I-80126 Napoli, Italy*
[50] *NIKHEF, National Institute for Nuclear Physics and High Energy Physics, NL-1009 DB Amsterdam, The Netherlands*
[51] *University of Notre Dame, Notre Dame, Indiana 46556, USA*
[52] *Ohio State University, Columbus, Ohio 43210, USA*
[53] *University of Oregon, Eugene, Oregon 97403, USA*
[54] *INFN Sezione di Padova[a]; Dipartimento di Fisica, Università di Padova[b], I-35131 Padova, Italy*
[55] *Laboratoire de Physique Nucléaire et de Hautes Energies, IN2P3/CNRS, Université Pierre et Marie Curie-Paris6, Université Denis Diderot-Paris7, F-75252 Paris, France*
[56] *INFN Sezione di Perugia[a]; Dipartimento di Fisica, Università di Perugia[b], I-06100 Perugia, Italy*

[57]INFN Sezione di Pisa[a]; Dipartimento di Fisica,
Università di Pisa[b]; Scuola Normale Superiore di Pisa[c], I-56127 Pisa, Italy
[58]Princeton University, Princeton, New Jersey 08544, USA
[59]INFN Sezione di Roma[a]; Dipartimento di Fisica,
Università di Roma La Sapienza[b], I-00185 Roma, Italy
[60]Universität Rostock, D-18051 Rostock, Germany
[61]Rutherford Appleton Laboratory, Chilton, Didcot, Oxon, OX11 0QX, United Kingdom
[62]CEA, Irfu, SPP, Centre de Saclay, F-91191 Gif-sur-Yvette, France
[63]SLAC National Accelerator Laboratory, Stanford, California 94309 USA
[64]University of South Carolina, Columbia, South Carolina 29208, USA
[65]Southern Methodist University, Dallas, Texas 75275, USA
[66]Stanford University, Stanford, California 94305-4060, USA
[67]State University of New York, Albany, New York 12222, USA
[68]Tel Aviv University, School of Physics and Astronomy, Tel Aviv, 69978, Israel
[69]University of Tennessee, Knoxville, Tennessee 37996, USA
[70]University of Texas at Austin, Austin, Texas 78712, USA
[71]University of Texas at Dallas, Richardson, Texas 75083, USA
[72]INFN Sezione di Torino[a]; Dipartimento di Fisica Sperimentale, Università di Torino[b], I-10125 Torino, Italy
[73]INFN Sezione di Trieste[a]; Dipartimento di Fisica, Università di Trieste[b], I-34127 Trieste, Italy
[74]IFIC, Universitat de Valencia-CSIC, E-46071 Valencia, Spain
[75]University of Victoria, Victoria, British Columbia, Canada V8W 3P6
[76]Department of Physics, University of Warwick, Coventry CV4 7AL, United Kingdom
[77]University of Wisconsin, Madison, Wisconsin 53706, USA

We have searched for the lepton-number violating processes $B^+ \to h^-\ell^+\ell^+$ with $h^- = K^-/\pi^-$ and $\ell^+ = e^+/\mu^+$, using a sample of 471 ± 3 million $B\overline{B}$ events collected with the *BABAR* detector at the PEP-II e^+e^- collider at the SLAC National Accelerator Laboratory. We find no evidence for these decays and place 90% confidence level upper limits on their branching fractions $\mathcal{B}\,(B^+ \to \pi^-e^+e^+) < 2.3 \times 10^{-8}$, $\mathcal{B}\,(B^+ \to K^-e^+e^+) < 3.0 \times 10^{-8}$, $\mathcal{B}\,(B^+ \to \pi^-\mu^+\mu^+) < 10.7 \times 10^{-8}$, and $\mathcal{B}\,(B^+ \to K^-\mu^+\mu^+) < 6.7 \times 10^{-8}$.

PACS numbers: 13.20.He,13.15.+g,14.60.St

In the Standard Model (SM), lepton number L is conserved in low-energy collisions and decays [1] and the lepton flavor numbers for the three lepton families are conserved if neutrinos are massless. The observation of neutrino oscillations [2] indicates that neutrinos have mass. If the neutrinos are of the Majorana type [3], the neutrino and antineutrino are the same particle and processes that involve lepton-number violation become possible. The lepton number must change by two units ($\Delta L = 2$) in this case and the most sensitive searches have so far involved neutrinoless nuclear double beta decays $0\nu\beta\beta$ [4]. The nuclear environment complicates the extraction of the neutrino mass scale. Processes involving meson decays have been proposed as an alternative that can also look for lepton-number violation with muons or τ leptons.

An example of a decay involving mesons is $B^+ \to h^-\ell^+\ell^+$, where $\ell^+ = e^+$ or μ^+ and h^- is a meson with a mass smaller than the B meson. A possible mechanism for this process involving the production and subsequent decay of a Majorana neutrino ν_m is illustrated in Fig. 1, which is topologically similar to the t-channel Feynman diagram in $0\nu\beta\beta$ decays. If the Majorana neutrino mass lies between the h meson and the B meson masses, resonance production could result in an enhanced peak in the invariant mass spectrum of the hadron and one of the leptons [5].

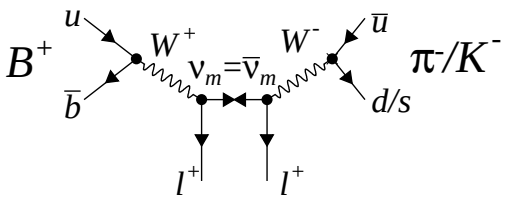

FIG. 1: An example diagram of the $\Delta L = 2$ process $B^+ \to h^-\ell^+\ell^+$ via s-channel Majorana neutrino ν_m production and decay.

The experimental approach in searches for these lepton-number violating processes is very similar to the approach for $B \to K^{(*)}\ell^+\ell^-$ and we use many of the techniques reported in Refs. [6, 7] to search for the four modes

*Now at the University of Tabuk, Tabuk 71491, Saudi Arabia
†Also with Università di Perugia, Dipartimento di Fisica, Perugia, Italy
‡Now at the University of Huddersfield, Huddersfield HD1 3DH, UK
§Now at University of South Alabama, Mobile, Alabama 36688, USA
¶Also with Università di Sassari, Sassari, Italy

$B^+ \to h^-\mu^+\mu^+$ and $B^+ \to h^-e^+e^+$, where $h^- = K^-$ or π^- (charge-conjugate modes are implied throughout this paper). Previous searches for these decays have produced 90% confidence level (C.L.) upper limits on the branching fractions in the range $(1.0 - 8.3) \times 10^{-6}$ [8]. The LHCb collaboration recently reported 95% C.L. upper limits on the branching fractions $\mathcal{B}(B^+ \to K^-\mu^+\mu^+) < 5.4 \times 10^{-8}$ and $\mathcal{B}(B^+ \to \pi^-\mu^+\mu^+) < 1.3 \times 10^{-8}$ [9]. The Belle collaboration place 90% C.L. upper limits on the branching fractions $\mathcal{B}(B^+ \to D^-\ell^+\ell^+)$ in the range $(1.1 - 2.6) \times 10^{-6}$ [10].

Our search uses a data sample of 471 ± 3 million $B\overline{B}$ pairs collected at the $\Upsilon(4S)$ resonance with the *BABAR* detector at the PEP-II asymmetric-energy e^+e^- collider at the SLAC National Accelerator Laboratory. The e^+e^- center-of-mass (CM) energy is $\sqrt{s} = 10.58\,\text{GeV}$, corresponding to the mass of the $\Upsilon(4S)$ resonance (on-resonance data). In addition, $43.9\,\text{fb}^{-1}$ of data collected 40 MeV below the $\Upsilon(4S)$ resonance (off-resonance data) are used for background studies. We assume equal production rates of B^+B^- and $B^0\overline{B}^0$ mesons [12]. The *BABAR* detector is described in detail in Ref. [11].

Monte Carlo (MC) simulation is used to evaluate the background contamination and selection efficiencies. The simulated backgrounds are also used to cross-check the selection procedure and for studies of systematic effects. The signal channels are simulated by the EvtGen [13] package using a three-body phase space model. We also generate light quark $q\overline{q}$ continuum events ($e^+e^- \to q\overline{q}$, $q = u, d, s, c$), di-muon, Bhabha elastic e^+e^- scattering, $B\overline{B}$ background and two-photon events [14]. Final-state radiation is provided by `Photos` [15]. The detector response is simulated with `GEANT4` [16], and all simulated events are reconstructed in the same manner as data.

We select events that have at least four charged tracks, the ratio of the second to zeroth Fox-Wolfram moments [17] less than 0.5, and two same-sign charged leptons each with momentum greater than $0.3\,\text{GeV}/c$ in the laboratory frame. The total transverse vector momentum of an event calculated in the laboratory frame must be less than $4\,\text{GeV}/c$; the distribution of this quantity peaks at $0.2\,\text{GeV}/c$ for signal events. The two leptons are constrained to come from a single vertex and an invariant mass $m_{\ell^+\ell^+} < 5.0\,\text{GeV}/c^2$ is required, to maintain compatibility with Ref. [6]. Electrons and positrons from photon conversions are removed, where photon conversion is indicated by electron-positron pairs with an invariant mass less than $0.03\,\text{GeV}/c^2$ and a production vertex more than 2 cm from the beam axis.

The charged pions and kaons are identified by measurements of their energy loss in the tracking detectors, the number of photons recorded by the ring-imaging Cherenkov detector and the corresponding Cherenkov angle. These measurements are combined with information from the electromagnetic calorimeter and the instrumented magnetic-flux return detector to identify electrons and muons [11].

The four-momenta of the electrons and positrons are corrected for Bremsstrahlung emission by searching for compatible photons. Using measurements made in the laboratory frame, the photon and electron four-momenta are combined if the photon energy E_γ is greater than $0.05\,\text{GeV}$, the shape of the energy deposit in the electromagnetic calorimeter is compatible with a photon shower, and the difference in polar angle between the photon and electron, measured at the point of closest approach to the beam spot, is less than 0.035 rad. In addition, the azimuthal angles ϕ of the photon ϕ_γ, the lepton ϕ_ℓ, and the calorimeter deposit associated with the lepton ϕ_c, all measured at the primary vertex, must be compatible with $\phi_\ell - 0.05 < \phi_\gamma < \phi_c$ for electrons and $\phi_c < \phi_\gamma < \phi_\ell + 0.05$ for positrons.

The two leptons and the hadron track are combined to form a B candidate. The B candidate is rejected if the invariant mass of the two leptons is in the range $2.85 < m_{\ell^+\ell^+} < 3.15\,\text{GeV}/c^2$ or $3.59 < m_{\ell^+\ell^+} < 3.77\,\text{GeV}/c^2$. Although a peaking background in the J/ψ or $\psi(2S)$ mass regions is not expected, these criteria maintain consistency with Ref. [6]. For the mode $B^+ \to \pi^-\mu^+\mu^+$, the invariant mass of each muon and the hadron must be outside the region $3.05 < m_{\ell^+h^-} < 3.13\,\text{GeV}/c^2$. This rejects events where a muon from a J/ψ decay is misidentified as a pion. The probability to misidentify a pion as a muon is of the order 2% and to misidentify as an electron less than 0.1%.

We measure the kinematic variables $m_{\rm ES} = \sqrt{s/4 - p_B^{*2}}$ and $\Delta E = E_B^* - \sqrt{s}/2$, where p_B^* and E_B^* are the B momentum and energy in the $\Upsilon(4S)$ CM frame, and $\sqrt{s}$ is the total CM energy. For signal events, the $m_{\rm ES}$ distribution peaks at the B meson mass with a resolution of about $2.5\,\text{MeV}/c^2$ and the ΔE distribution peaks near zero with a resolution of about 20 MeV, indicating that the candidate system of particles has total energy consistent with the beam energy in the CM frame. The B candidate is required to be in the kinematic region $5.200 < m_{\rm ES} < 5.289\,\text{GeV}/c^2$ and $-0.10 < \Delta E < 0.05\,\text{GeV}$.

The main backgrounds arise from light quark $q\overline{q}$ continuum events and $B\overline{B}$ backgrounds formed from random combinations of leptons from semileptonic B and D decays. These are suppressed through the use of boosted decision tree discriminants (BDTs) [18]. As the input variable distributions for the $q\overline{q}$ continuum and the $B\overline{B}$ backgrounds are sufficiently different, two BDTs are trained, one to distinguish between signal and $q\overline{q}$ continuum, and the other between signal and $B\overline{B}$ backgrounds. Each BDT is trained in four regions according to lepton type (muon versus electron) and mass range ($m_{\ell^+\ell^+}$ above or below the J/ψ mass). The input variables consist of ΔE and seventeen parameters that represent the event shape of the decay, the distance of closest approach of the di-lepton system to the beam axis, the vertex probabilities of the di-lepton and B candidates, the magnitudes of the thrusts of both the decay particles and the rest of the event, and the thrust directions with respect to the beam axis of the experiment.

To construct the BDTs, we use simulated samples of events for the signal and background, and we assume background decay rates consistent with measured values [19]. We compare the distributions of the data and the simulated background variables used as input to the BDTs and confirm that they are consistent.

The output distributions of the $q\overline{q}$ and $B\overline{B}$ BDTs are each used to define probability distribution functions $\mathcal{P}_{\rm sig}$ and $\mathcal{P}_{\rm bkg}$ for signal and background, respectively. The probabilities are used to define a likelihood ratio $\mathcal{R}$ as

$$\mathcal{R} \equiv \frac{\mathcal{P}_{\rm sig}^{B\overline{B}} + \mathcal{P}_{\rm sig}^{q\overline{q}}}{\mathcal{P}_{\rm sig}^{B\overline{B}} + \mathcal{P}_{\rm sig}^{q\overline{q}} + \mathcal{P}_{\rm bkg}^{B\overline{B}} + \mathcal{P}_{\rm bkg}^{q\overline{q}}}. \quad (1)$$

We veto candidates if either $\mathcal{P}_{\rm sig}^{B\overline{B}}$ or $\mathcal{P}_{\rm sig}^{q\overline{q}}$ is less than 0.5 or the ratio $\mathcal{R}$ less than 0.2. This retains 85% of the simulated signal events while rejecting more than 95% of the background.

After the application of all selection criteria, some events will contain more than one reconstructed B candidate. Fewer than 1% of accepted events have more than one B candidate. We select the most probable B candidate from among all the candidates in the event using the likelihood ratio $\mathcal{R}$. Averaged over all events, the correct B candidate in simulated signal events is selected with greater than 98.5% accuracy. For events with more than one B candidate, the correct candidate is selected with an accuracy of 67%-82% depending on the mode. The final event selection efficiency for simulated signal is 13%-48% depending on the final state. The selection efficiency for all modes is approximately constant to within a relative $\pm 10\%$ as a function of $m_{\ell^+h^-}$ between m_{h^-} and $4.6\,{\rm GeV}/c^2$.

We extract the signal and background yields from the data with an unbinned maximum likelihood (ML) fit using

$$\mathcal{L} = \frac{1}{N!}\exp\left(-\sum_j n_j\right)\prod_{i=1}^{N}\left[\sum_j n_j \mathcal{P}_j(\vec{x}_i;\vec{\alpha}_j)\right], \quad (2)$$

where the likelihood $\mathcal{L}$ for each event candidate i is the sum of $n_j\mathcal{P}_j(\vec{x}_i;\vec{\alpha}_j)$ over two categories j: the signal mode $B^+ \to h^-\ell^+\ell^+$ (including the small number of misreconstructed B candidates) and background as discussed below. For each category j, $\mathcal{P}_j(\vec{x}_i;\vec{\alpha}_j)$ is the product of the probability density functions (PDFs) evaluated for the i-th event's measured variables $\vec{x}_i$. The number of events for category j is denoted by n_j and N is the total number of events in the sample. The quantities $\vec{\alpha}_j$ represent the parameters describing the expected distributions of the measured variables for each category j. Each discriminating variable $\vec{x}_i$ in the likelihood function is modeled with a PDF, where the parameters $\vec{\alpha}_j$ are extracted from MC simulation, off-resonance data, or on-resonance data with $m_{\rm ES} < 5.27\,{\rm GeV}/c^2$. The two variables $\vec{x}_i$ used in the fit are $m_{\rm ES}$ and $\mathcal{R}$. Since the linear correlations between the two variables are found to be only 4%-7% for simulated signal modes and 8%-12% for simulated background and on-resonance data, we take each $\mathcal{P}_j$ to be the product of the PDFs for the separate variables. Any correlations in the variables are treated later as a systematic uncertainty. The three free parameters in the fit are the numbers of signal and background events and the slope of the background $m_{\rm ES}$ distribution.

MC simulations show that the $q\overline{q}$ and $B\overline{B}$ backgrounds have very similar distributions in $m_{\rm ES}$ and $\mathcal{R}$. We therefore use a single ARGUS shape [20] to describe the $m_{\rm ES}$ combinatorial background, allowing the shape parameter to float in the fits. The ratio $\mathcal{R}$ for both signal and background is fitted using a non-parametric kernel estimation KEYS algorithm [21].

We parameterize the signal $m_{\rm ES}$ distributions using a Gaussian shape unique to each final state, with the mean and width determined from fits to the analogous final states in the $B^+ \to J/\psi(\to \ell^+\ell^-)h^+$ events from the on-resonance data. The same selection criteria as given above are used, with the modification that two opposite-sign leptons are required, the reconstructed J/ψ mass must be in the range 2.95 to $3.15\,{\rm GeV}/c^2$, $m_{\rm ES}$ greater than $5.24\,{\rm GeV}/c^2$, and ΔE between -0.3 and $0.2\,{\rm GeV}$. The signal and background $m_{\rm ES}$ on-resonance data distributions are fitted with a Gaussian and an ARGUS function, respectively. For modes with a pion in the final state, we account for $J/\psi K^+$ misidentified as $J/\psi\pi^+$ by using the signal distribution extracted from the $J/\psi K^+$ data as an additional background. For both $J/\psi \to e^+e^-$ and $J/\psi \to \mu^+\mu^-$, the J/ψ mass distribution has a width $\sim 15\,{\rm MeV}/c^2$. The $m_{\rm ES}$ mean for all modes is $5.2791 \pm 0.0001\,{\rm GeV}/c^2$ and the width is $(2.41 - 2.56)$ ${\rm MeV}/c^2$ with an error $(0.02 - 0.09)$ ${\rm MeV}/c^2$, depending on the mode. The means and widths are robust against changes in the assumptions concerning the relative contribution of $q\overline{q}$ and $B\overline{B}$ events to the backgrounds and the functions used to fit the signal and background distributions. The numbers of measured events for the four modes are within one standard deviation of the expected numbers calculated from previously measured branching fractions [12]. Figure 2 shows the extracted $m_{\rm ES}$ distributions for each mode.

As a cross-check of the background PDFs to $B^+ \to h^-\ell^+\ell^+$, we perform a fit to a simulated background sample, with the same number of events as the on-resonance data sample, and also a fit to the off-resonance data sample. In both cases, the number of signal events is compatible with zero for all four modes.

We test the performance of the fits to $B^+ \to h^-\ell^+\ell^+$ by generating ensembles of MC datasets from both the PDF distributions and the fully simulated MC events. The mean number of signal and background events used in the ensembles is taken from the full default model fit to the selected on-resonance data sample described above. We generate and fit 5000 datasets with the number of signal and background events allowed to fluctuate according

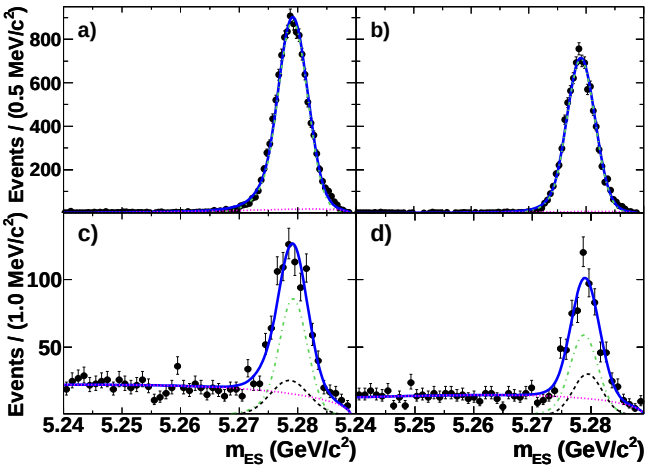

FIG. 2: The $m_{\rm ES}$ distributions for a) $B^+ \to J/\psi(\to e^+e^-)K^+$; b) $B^+ \to J/\psi(\to \mu^+\mu^-)K^+$; c) $B^+ \to J/\psi(\to e^+e^-)\pi^+$; and d) $B^+ \to J/\psi(\to \mu^+\mu^-)\pi^+$. The solid (blue) line is the total fit, the dotted (magenta) line is the background, the dash-dotted (green) line is the signal, the dashed (black) line is the misidentified $J/\psi\, K^+$ events.

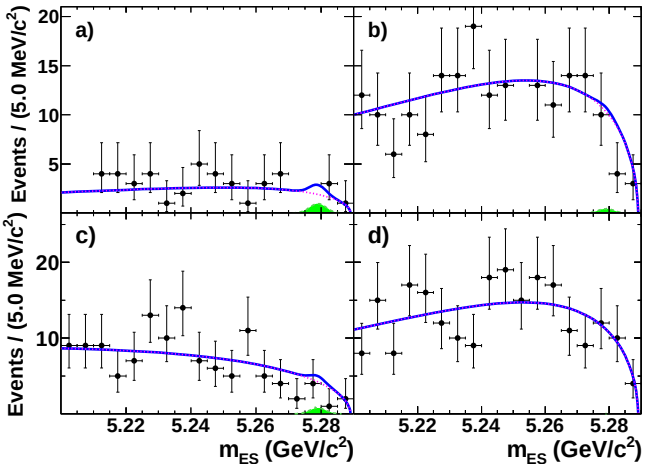

FIG. 3: The $m_{\rm ES}$ distributions for a) $B^+ \to K^-e^+e^+$; b) $B^+ \to K^-\mu^+\mu^+$; c) $B^+ \to \pi^-e^+e^+$; and d) $B^+ \to \pi^-\mu^+\mu^+$. The solid (blue) line is the total fit, the dotted (magenta) line is the background, the solid (green) histogram is the signal.

to a Poisson distribution. The signal yield bias in the ensemble of fits is between -0.30 and 0.15 events, depending on the mode, and this is subtracted from the yield taken from the data.

The results of the ML fits to the on-resonance data are summarized in Table I. Figure 3 shows the $m_{\rm ES}$ distributions for the four modes. The signal significance is defined as $\mathcal{S} = \sqrt{2\Delta \ln \mathcal{L}}$, where $\Delta \ln \mathcal{L}$ is the change in log-likelihood from the maximum value to the value when the number of signal events is set to zero. Systematic errors are included in the log-likelihood distribution by convolving the likelihood function with a Gaussian distribution with a variance equal to the total systematic error defined below. The branching fraction $\mathcal{B}$ is given by $n_s/(\eta N_{B\overline{B}})$ where n_s is the signal yield, corrected for the fit bias, η is the reconstruction efficiency and $N_{B\overline{B}}$ is the number of $B\overline{B}$ events collected.

The systematic uncertainties in the branching fractions are summarized in Table II. They arise from the PDF parameterization, fit biases, background yields, and efficiencies. The PDF uncertainties are calculated by varying, by their errors, the PDF parameters that are held fixed in the default fit, taking into account correlations. For the non-parametric kernel estimation KEYS algorithm, we vary the smearing parameter between 50% and 200% of the nominal value. The uncertainty from the fit bias includes the statistical uncertainty from the simulated experiments and half of the correction itself, added in quadrature.

Two tests are used to calculate the contribution to the error caused by the assumption that the $q\overline{q}$ and $B\overline{B}$ backgrounds have similar distributions. We first vary the relative proportions of light quark $q\overline{q}$, $c\overline{c}$, and $B\overline{B}$ used in the simulated background between 0% and 100%. The new simulated background $\mathcal{R}$ PDF is then used in the fit to the data and compared to the default fit to data. We also perform an ensemble of fits to MC samples consisting of one simulated signal event and the number of simulated background events given by the default fit to data. The relative proportions of light quark $q\overline{q}$, $c\overline{c}$, and $B\overline{B}$ in the simulated background are varied and a fit performed to the MC sample. The result is compared to the fit to the default MC sample. The error is calculated as half the difference between the default fit and the maximum deviation seen in the ensemble of fits. All these errors described above are additive in nature and affect the significance of the branching fraction results.

Multiplicative uncertainties include reconstruction efficiency uncertainties from tracking (0.8% per track added linearly for the leptons and 0.7% for the kaon or pion), charged lepton particle identification (0.7% per track added linearly for electrons, 1.0% for muons), hadron particle identification (0.2% for pions, 0.6% for kaons), uncertainty in the BDT response from comparison to charmonium control samples (2.0%), the number of $B\overline{B}$ pairs (0.6%), and MC signal statistics (0.2%). The total multiplicative branching fraction uncertainty is 3.2% or less for all modes.

As shown in Table I, we observe no significant yields. The 90% C.L. branching fraction upper limits $\mathcal{B}_{UL}$ are determined by integrating the total likelihood distribution (taking into account statistical and systematic errors) as a function of the branching fraction from 0 to $\mathcal{B}_{UL}$, such that $\int_0^{\mathcal{B}_{UL}} \mathcal{L}d\mathcal{B} = 0.9 \times \int_0^{\infty} \mathcal{L}d\mathcal{B}$. The upper limits are dominated by the statistical error.

Figure 4 shows $\mathcal{B}_{UL}$ as a function of the mass $m_{\ell^+h^-}$

TABLE I: Results for the measured B decays, showing the total events in the sample, signal yield fit bias (with error), signal yield (corrected for fit bias) and its statistical uncertainty, reconstruction efficiency η, significance $\mathcal{S}$ (with statistical and systematic uncertainties included), branching fraction $\mathcal{B}$, and 90% C.L. branching fraction upper limits $\mathcal{B}_{UL}$.

Mode	Events	Fit Bias	Yield	η (%)	$\mathcal{S}$ (σ)	$\mathcal{B}$ ($\times 10^{-8}$)	$\mathcal{B}_{UL}$ ($\times 10^{-8}$)
$B^+ \to \pi^- e^+ e^+$	123	$+0.15 \pm 0.09$	$0.6^{+2.5}_{-2.7}$	47.8 ± 0.1	0.4	$0.27^{+1.1}_{-1.2} \pm 0.1$	2.3
$B^+ \to K^- e^+ e^+$	42	-0.30 ± 0.15	$0.7^{+1.8}_{-1.2}$	30.9 ± 0.1	0.5	$0.49^{+1.3}_{-0.8} \pm 0.1$	3.0
$B^+ \to \pi^- \mu^+ \mu^+$	228	-0.01 ± 0.05	$0.0^{+3.2}_{-2.0}$	13.1 ± 0.1	0.0	$0.03^{+5.1}_{-3.2} \pm 0.6$	10.7
$B^+ \to K^- \mu^+ \mu^+$	209	$+0.02 \pm 0.04$	$0.5^{+3.5}_{-2.5}$	23.0 ± 0.1	0.2	$0.45^{+3.2}_{-2.7} \pm 0.4$	6.7

TABLE II: Summary of branching fraction $\mathcal{B}$ systematic uncertainties for the four decays.

Systematic	$\pi^- e^+ e^+$	$K^- e^+ e^+$	$\pi^- \mu^+ \mu^+$	$K^- \mu^+ \mu^+$
Additive uncertainties (candidates)				
PDF variation	0.01	0.01	0.01	0.09
KEYS PDFs	0.30	0.05	0.23	0.02
Fit bias	0.09	0.15	0.05	0.04
Backgrounds	0.05	0.07	0.25	0.35
Total	0.32	0.17	0.34	0.35
Multiplicative uncertainties (%)				
Lepton tracking	1.6	1.6	1.6	1.6
Hadron tracking	1.4	1.4	1.4	1.4
Lepton ID	0.7	0.7	1.0	1.0
Hadron ID	0.2	0.6	0.2	0.6
BDT	2.0	2.0	2.0	2.0
$B\overline{B}$ pairs	0.6	0.6	0.6	0.6
MC statistics	0.2	0.2	0.2	0.2
Total	3.1	3.1	3.2	3.2
Branching fraction $\mathcal{B}$ uncertainties ($\times 10^{-8}$)				
Additive	0.14	0.12	0.56	0.34
Multiplicative	0.01	0.02	0.01	0.01
Total	0.14	0.12	0.56	0.35

for the four modes. The $\mathcal{B}_{UL}$ limit is recalculated in bins of 0.1 GeV/c^2 with the assumption that all the fitted signal events are contained in that bin. The total likelihood distribution from the default fit is rescaled taking into account the reconstruction efficiency in each $m_{\ell^+h^-}$ bin and the increased uncertainty in the estimate of the reconstruction efficiency due to reduced MC statistics. The $\mathcal{B}_{UL}$ limit in each $m_{\ell^+h^-}$ bin is then recalculated using the formula given above. The change in shape is mainly due to the variation of the reconstruction efficiency as a function of the mass. If the decay $B^+ \to h^- \ell^+ \ell^+$ is caused by the exchange of a Majorana neutrino, as illustrated in Fig. 1, then $m_{\ell^+h^-}$ can be related to the Majorana neutrino mass m_ν [5].

In summary, we have searched for the four lepton-number violating processes $B^+ \to h^- \ell^+ \ell^+$. We find no significant yields and place 90% C.L. upper limits on the branching fractions in the range $(2.3 - 10.7) \times 10^{-8}$. The

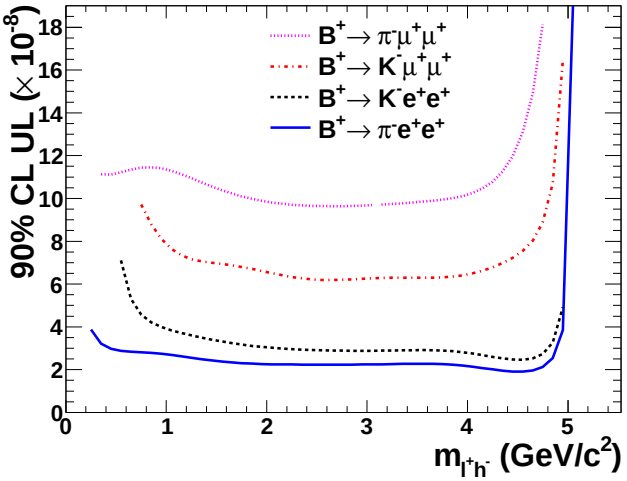

FIG. 4: 90% C.L. upper limits on the branching fraction as a function of the mass $m_{\ell^+h^-}$ for $B^+ \to \pi^- \mu^+ \mu^+$ (dotted/magenta line), $B^+ \to K^- \mu^+ \mu^+$ (dash-dotted/red line), $B^+ \to K^- e^+ e^+$ (dashed/black line), and $B^+ \to \pi^- e^+ e^+$ (solid/blue line).

branching fraction upper limit for $B^+ \to \pi^- \mu^+ \mu^+$ is less restrictive than the result reported in Ref. [9], while the $B^+ \to K^- \mu^+ \mu^+$ limit is commensurate. The limits for $B^+ \to K^- e^+ e^+$ and $B^+ \to \pi^- e^+ e^+$ are 30 and 70 times more stringent, respectively, than previous measurements at $e^+ e^-$ colliders [8].

We are grateful for the excellent luminosity and machine conditions provided by our PEP-II colleagues, and for the substantial dedicated effort from the computing organizations that support *BABAR*. The collaborating institutions wish to thank SLAC for its support and kind hospitality. This work is supported by DOE and NSF (USA), NSERC (Canada), CEA and CNRS-IN2P3 (France), BMBF and DFG (Germany), INFN (Italy), FOM (The Netherlands), NFR (Norway), MES (Russia), MICIIN (Spain), STFC (United Kingdom). Individuals have received support from the Marie Curie EIF (European Union) and the A. P. Sloan Foundation (USA).

[1] F.R. Klinkhamer and N.S. Manton, Phys. Rev. D **30**, 2212 (1984).

[2] G.L. Fogli, E. Lisi, A. Marrone, A. Palazzo, and A.M. Rotunno, Phys. Rev. D **84**, 053007 (2011).

[3] E. Majorana, Nuo. Cim. **14**, 171-184 (1937).

[4] J.J. Gomez-Cadenas *et al.*, submitted to La Rivista del Nuovo Cimento, arXiv:1109.5515.

[5] J.-M. Zhang and G.-L. Wang, Eur. Phys. Jour. C **71**, 1715 (2011); A. Atre, T. Han, S. Pascali, and B. Zhang, JHEP 0905:030 (2009); T. Han and B. Zhang, Phys. Rev. Lett. **97**, 171804 (2006).

[6] B. Aubert *et al.* (*BABAR* Collaboration), Phys. Rev. D **79**, 031102 (2009).

[7] B. Aubert *et al.* (*BABAR* Collaboration), Phys. Rev. Lett. **102**, 091803 (2009); B. Aubert *et al.* (*BABAR* Collaboration), Phys. Rev. D **73**, 092001 (2006).

[8] K. W. Edwards *et al.* (CLEO Collaboration), Phys. Rev. D **65**, 111102 (2002).

[9] R. Aaij *et al.* (LHCb Collaboration), CERN-PH-EP-2011-156, arXiv:1110.0730; R. Aaij *et al.* (LHCb Collaboration), CERN-PH-EP-2012-006, arXiv:1201.5600.

[10] O. Seon *et al.* (Belle Collaboration), Phys. Rev. D **84**, 071106 (2011).

[11] B. Aubert *et al.* (*BABAR* Collaboration), Nucl. Instrum. Methods Phys. Res., Sect. A **479**, 1 (2002).

[12] K. Nakamura *et al.* (Particle Data Group), J. Phys. **G37**, 075021 (2010) and 2011 partial update for the 2012 edition.

[13] D. J. Lange, Nucl. Instrum. Methods Phys. Res., Sect. A **462**, 152 (2001).

[14] B. F. Ward, S. Jadach, and Z. Was, Nucl. Phys. Proc. Suppl. **116**, 73 (2003); T. Sjöstrand, Comput. Phys. Commun. **82**, 74 (1994).

[15] E. Barberio and Z. Was, Comput. Phys. Commun. **79**, 291 (1994).

[16] S. Agostinelli *et al.*, (GEANT4 Collaboration), Nucl. Instrum. Methods Phys. Res., Sect. A **506**, 250 (2003).

[17] G. C. Fox and S. Wolfram, Nucl. Phys. B **157**, 543 (1979).

[18] B. P. Roe *et al.*, Nucl. Instrum. Methods Phys. Res., Sect. A **543**, 577 (2005).

[19] Heavy Flavor Averaging Group, D. Asner *et al.*, arXiv:1010.1589 (2010).

[20] H. Albrecht *et al.* (ARGUS Collaboration), Z. Phys. C **48**, 543 (1990).

[21] K. S. Kramer, Comput. Phys. Commun. **136**, 198 (2001).